Teruel-Juanes, R.; Pascual-Jose, B.; Del Río, C.; García, O.; Ribes-Greus, A. (2020). Dielectric analysis of photocrosslinked and post-sulfonated styrene-ethylene-butylene-styrene block copolymer based membranes. Reactive and Functional Polymers. 155:1-11. https://doi.org/10.1016/j.reactfunctpolym.2020.104715

R. Teruel-Juanes, B. Pascual-Jose, C. del Río, O. García, A. Ribes-Greus. Dielectric analysis of photocrosslinked and post-sulfonated styrene-ethylene-butylene-styrene block copolymer based membranes. Reactive and Functional Polymers 2020; 155:104715

DIELECTRIC ANALYSIS OF PHOTOCROSSLINKED AND POST-SULFONATED STYRENE-ETHYLENE-BUTYLENE-STYRENE BLOCK COPOLYMER BASED MEMBRANES

R. Teruel-Juanes[1], B. Pascual-Jose[1], C. del Río[2], O. García[2], A. Ribes-Greus[1,*]

[1] Institute of Technology of Materials (ITM), Universitat Politècnica de València (UPV), Camí de Vera, s/n, 46022, Spain.

[2] Institute of Polymer Science and Technology (ICTP-CSIC), Juan de la Cierva 3, 28006 Madrid, Spain.

***Corresponding author: A. Ribes-Greus** aribes@ter.upv.es

R. Teruel-Juanes, B. Pascual-Jose, C. del Río, O. García, A. Ribes-Greus. Dielectric analysis of photocrosslinked and post-sulfonated styrene-ethylene-butylene-styrene block copolymer based membranes. Reactive and Functional Polymers 2020; 155:104715

DIELECTRIC ANALYSIS OF PHOTOCROSSLINKED AND POST-SULFONATED STYRENE-ETHYLENE-BUTYLENE-STYRENE BLOCK COPOLYMER BASED MEMBRANES

R. Teruel-Juanes[1], B. Pascual-Jose[1], C. del Río[2], O. García[2], A. Ribes-Greus[1,*]

[1] Institute of Technology of Materials (ITM), Universitat Politècnica de València (UPV), Camí de Vera, s/n, 46022 , Spain.

[2] Institute of Polymer Science and Technology (ICTP-CSIC), Juan de la Cierva 3, 28006 Madrid, Spain.

***Corresponding author: A. Ribes-Greus** aribes@ter.upv.es

Abstract

A series of UV photocrosslinked and post-sulfonated membranes based on blends of styrene-ethylene-butylene-styrene triblock copolymer (SEBS) and divinylbenzene (DVB) were considered for the preparation of electrolytes for proton exchange membrane fuel cell (PEMFC) applications. Macromolecular dynamics of SEBS and SEBS-DVB membranes below and above the T_g, were analysed using dielectric thermal analysis (DETA). A sub-*Tg* intramolecular non-cooperative dielectric relaxation and two main relaxations, corresponding to the glass transitions of ethylene-butylene (EB) and styrene (S) blocks, were identified in the dielectric relaxation spectrum. The photocrosslinking and post-sulfonation processes affect to the entire dielectric relaxation spectrum, the apparent activation energy and the fragilities of both styrene (S) and ethylene-butylene (EB) blocks. Understanding the restrictions on the segmental mobility at low and high scale caused by both photocrosslinking and subsequent sulfonation is basic to provide an approach to ionic diffusivities.

A correlation between relaxations processes and the performance of these membranes in H_2/O_2 - PEM single cells allows to estimate the behaviour of these membranes and to reengineer them, depending on the modification of the desired cell performance.

R. Teruel-Juanes, B. Pascual-Jose, C. del Río, O. García, A. Ribes-Greus. Dielectric analysis of photocrosslinked and post-sulfonated styrene-ethylene-butylene-styrene block copolymer based membranes. Reactive and Functional Polymers 2020; 155:104715

Keywords

Photocrosslinking
Post-sulfonated SEBS membranes
Dielectric relaxation properties
Segmental dynamics
Proton exchange membrane fuel cells

Highlights

- Detailed information about the molecular dynamics of these membranes is offered.
- The photocrosslinking straitens the chain mobility hindering the ionic diffusion.
- Low degrees of sulfonation improve the ionic mobility of the membranes.
- DETA is found to be a valid experimental technique for fine-tuning membranes.

Graphical Abstract

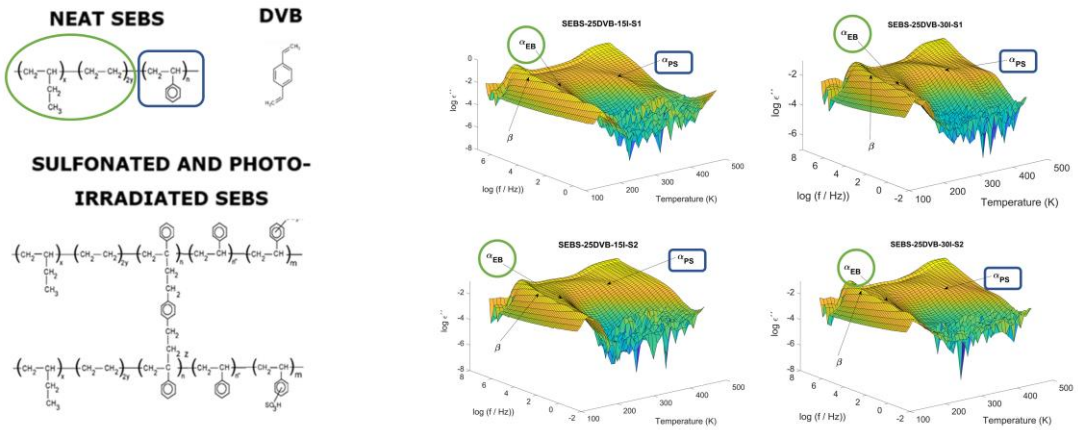

1. Introduction

Proton exchange membrane fuel cells (PEMFC) are eco-friendly devices for the production of an environmental sustainable energy [1–3]. The overall performance and efficiency of these fuel cells are closely related to the proton conductivity and dimensional stability of the membranes used as electrolytes. These membranes are typically a phase separated material, which acts as a selective barrier, where the hydrophobic phase gives mechanical stability and the hydrophilic domain regulates proton exchange.

Many studies have been devoted to developing new membrane materials presenting a suitable dimensional stability, high ionic conductivity and low cost for a significant volume production, among them, block copolymer ionomers based on styrenic thermoplastic elastomers bearing sulfonic acid groups. The introduction of ionic groups into the polystyrene blocks causes significant changes in many physical properties, not only the emergence of ionic conductivity but also changes in hydrophilicity, mechanical strength and glass transition temperature which are not detected in their non-ionic counterparts [4–8].

The interest in polystyrene multiblock copolymers as polymer electrolytes for fuel cell applications is mainly due to their ability to form ion conducting channels as a consequence of their phase-separated morphology [9–11]. Additionally, its sulfonation might offer more useful features such a low methanol permeability or a higher mechanical stability. SEBS (styrene-ethylene-butylene-styrene) triblock copolymer is a commercial and economical material widely studied, which is obtained by hydrogenation of the thermoplastic elastomer of styrene and butadiene, eliminating the unsaturation of the butylene chain. In this work, SEBS has been chosen as the base material because it has properties such as resistance to the environment, temperature, UV (ultraviolet) radiation, etc. After sulfonation, via electrophilic substitution, a nanometre scale phase separated morphology of hydrophilic and hydrophobic domains is generated providing proton mobility paths in wet state which makes sulfonated SEBS (sSEBS) very attractive for its use in fuel cells [12–16].

Unfortunately, a high degree of sulfonation is often required to achieve suitable proton conductivity, which causes excessive swelling in water with the consequent loss of mechanical resistance and poor cell performance. In a previous work, photocrosslinking and post-sulfonation of membranes based on mixtures of SEBS and divinylbenzene (DVB) were successfully used to overcome these stability limitations. It was found that both the degree of photoirradiation and post-sulfonation modified the sizes and geometries of the separated nanostructure, and subsequently, the mobility of the molecular chains, which affected the proton conductivity and the behaviour of these membranes as electrolytes in the PEMFC [17].

Dielectric thermal analysis (DETA) is a powerful and sensitive tool for analysing macromolecular dynamics. These studies are especially interesting in these heterogeneous polymers with separated phases due to the interfaces. Thus, when analysing the spectrum of dielectric relaxations, it is possible to provide some data on the distribution of the blocks and their effect on the molecular movements of the polymer chains that constitute them [18–24]. In particular, the dielectric spectra of SEBS is found to display a very low response, being almost frequently independent due to its nonpolar nature [25–27]. Chen et al. studied the dielectric spectrum of neat and sulfonated SEBS with different degrees of sulfonation. The dielectric spectra was found to display three molecular relaxations corresponding to local chain motions, the glass transition of the ethylene-butylene block and the glass transition of the styrene block, respectively. Sulfonation was found to shift the glass transition temperature of both blocks [20]. From these studies it can be inferred that polymers with phase separation form gradients of dielectric permittivity, that modify the overall behaviour as selective transport media when these materials work as an electrolyte.

Dielectric thermal analysis has been performed to understand the molecular mobility as a function of photocrosslinking and the degree of sulfonation. Thus, the dielectric relaxation spectrum was studied as a function of the temperature and frequency below and near the polymer glass transition temperature T_g, to know the molecular mobility

and reach with the ionic diffusion. The Havriliak–Negami model was used to model the relaxation processes, to obtain the relaxation parameters. The correlation between DETA results and H_2/O_2 performance are relevant for the reengineering of the electrolytes. The obtained results allow the establishment of the operating relationships, which underlie the new design strategies of anisotropic electrolytes applicable for proton exchange membrane fuel cells (PEMFC).

2. Experimental procedure

2.1. Materials

The starting material SEBS (styrene-ethylene-butylene-styrene block copolymer) used in this study was Calprene CH-6120 (Repsol) with 32wt.% by weight of styrene units.
Other chemicals products were divinylbenzene (DVB, Sigma-Aldrich) as photocrosslinkable monomer; Irgacure 651 (IRG 651-2,2-dimethoxy-1,2-diphenylethan-1-one) (Ciba) as a photoinitiator; trimethylsilyl chlorosulfonate (99%, Sigma - Aldrich) as a sulfonation reagent; Chloroform ($CHCl_3$-, Scharlau); 1,2-dichloroethane (DCE, Scharlau) as solvents; all of them were employed as received without any further treatment of purification.

2.2 Membrane preparation: photocrosslinking and post-sulfonation

The membranes were prepared using doctor Blade from chloroform solutions by mixing SEBS with 25% by weight of photocrosslinkable divinylbenzene (DVB) and 2% of photoinitiator based on the weight of DVB. After drying, the membranes were UV irradiated (Hamamatsu L8868) for 15 and 30 minutes. The sulfonation was performed using trimethylsilyl chlorosulfonate solutions in DCE (0.3 M 2 hours and 0.5 M 3 hours). The processes of membrane preparation, photocrosslinking and post-sulfonation were described in more detail elsewhere [17]. The different chemical structures are illustrated in **Figure 1** and **Table 1** shows the membrane nomenclature used according to the different experimental conditions.

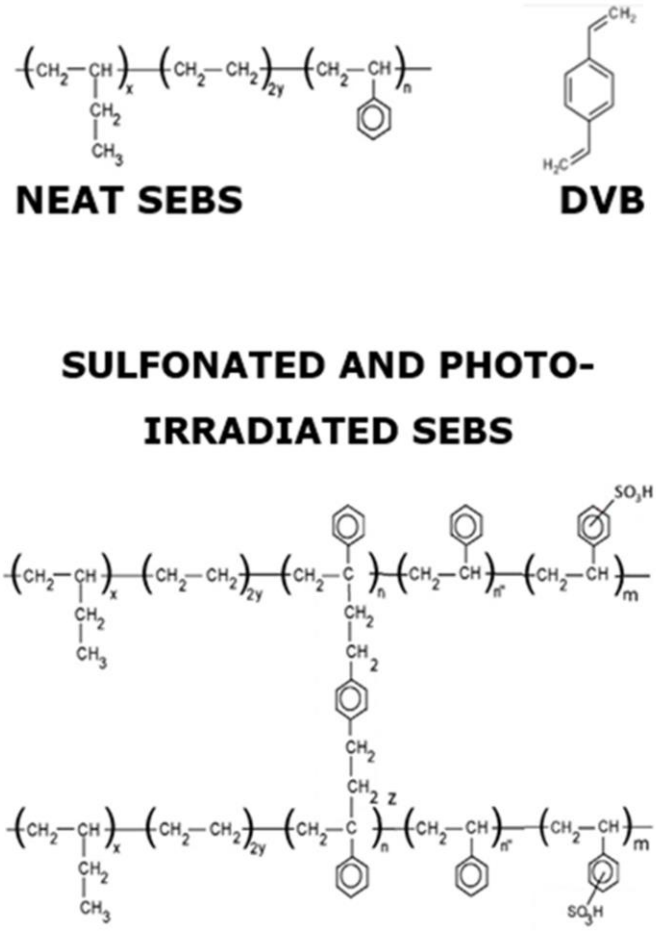

Figure 1

Table 1

UV Irradiation (min)	Sulfonation	Label
-	-	SEBS
-	-	SEBS-25DVB
15	-	SEBS-25DVB-15I
	0.3 M for 2 h	SEBS-25DVB-15I-S1
	0.5 M for 3 h	SEBS-25DVB-15I-S2
30	-	SEBS-25DVB-30I
	0.3 M for 2 h	SEBS-25DVB-30I-S1
	0.5 M for 3 h	SEBS-25DVB-30I-S2

2.3. Dynamic Dielectric Thermal Analysis (DETA) assessment

The dielectric relaxation spectra of all the membranes was measured under isothermal conditions by using a Dielectric Spectrometer of Novocontrol Technologies GmbH & Co. KG, at the frequency range f = 10^{-2} - 10^{7} Hz. The measurements were carried out in inert N_2 atmosphere from 123 to 473 K in increasing steps of 10 K. Dielectric experiments were performed in a cell constituted by two gold electrodes were the sample electrode assembly (SEA), consisting of two stainless steel electrodes, was located. A Teflon® film was inserted between the sample and one steel electrode only if the conductivity is too high that overlaps the relaxations.

The dielectric relaxation complex spectra were described using the empirical Havriliak–Negami (HN) functions. The observed relaxations spectra were deconvolved applying Charlesworth's method, adding as many Havriliak-Negami equations as necessary. All the characteristic parameters of each relaxation process were determinate [28–30].

$$\varepsilon^*(w) - \varepsilon_\infty = \sum_k \mathrm{Im}\left[\frac{\Delta\varepsilon}{\left\{1 + (iw\tau_{HNk})^{a_k}\right\}^{b_k}}\right] \qquad (Eq.1)$$

Where:

τ_{HN} is the Havriliak-Negami relaxation time. Thus, the sub index *k* represents the number of the individual HN contributions.

a and *b* are parameters corresponding to the width and asymmetry broadening of the relaxation peak of the relaxation time distributions.

$\Delta\varepsilon$ is the value of the dielectric intensity or relaxation strength.

2.4. Proton conductivity measurements

Through-plane proton conductivities of the membranes were determined by means of electrochemical impedance spectroscopy (EIS) using a potentiostat Autolab PGStat30. The cell was heated at 333 K and supplied with humidified gases (hydrogen, SHE anode; nitrogen, cathode) with a continuous flow of 200 $mL \cdot min^{-1}$. The falling frequency range was from 10 kHz to 1 Hz with amplitude of the sinusoidal signal of 10 mV. The through-plane proton conductivity σ_{TP} ($S \cdot cm^{-1}$) was determined using the **Equation 2**:

$$\sigma_{TP} = L / R_m S \qquad (Eq.\ 2)$$

where *L* is the thickness of the membrane (cm) and *S* is the active area (5 cm^2). The membrane resistance R_m (Ω) was measured at the frequency that produced the minimum imaginary response. Each sample was measured at least five times until a constant resistance value was reached.

3. Results and discussion

The dielectric relaxation spectra of membranes prepared with styrene-ethylene-butylene-styrene block copolymer (SEBS), mixed with divinylbenzene (DVB), photocrosslinked and subsequently sulfonated with different degrees of sulfonation were analyzed. The spectra were plotted in terms of the real ε' and imaginary ε'' parts of the complex dielectric permittivity ε*, for a given set of temperatures and frequencies.

Figure 2 plots the dielectric relaxation spectrum in 3D of the photocrosslinked and sulfonated copolymers in terms of the imaginary ε'' component of the complex dielectric permittivity ε^* at the frequency range $f = 10^{-2}$ - 10^{7} Hz in a wide range of temperatures. The spectra of the SEBS copolymers consists of several relaxation processes that correspond to molecular motions of some atoms of the backbone, lateral chain or glass transition of each block. At higher temperature and frequencies, external electrode polarization, interfacial polarization (Maxwell-Wagner-Sillars) and conductivity may be observed overlapped to the relaxation spectrum. Thus, it is difficult to differentiate between interfacial peaks and the true relaxation processes that take place in a heterogeneous media. As the separation of charges is the molecular origin of this phenomenon and it is not related to backbone molecular movements, in this study it is not analysed as a relaxation process.

Figure 2 shows different zones of relaxation: a weak relaxation zone at low temperature attributed to β relaxation as resulted from the movement in which participate a number of few atoms from the main or the lateral chain. That is, the reorientation of small angles in relation to the longitudinal axis of the polymer in corresponding poly(ethylene-butylene) (PEB) block [21].

At higher temperatures, two additional relaxations are observed, which may be related to both components of the block copolymer: ethylene-butylene and styrene. These relaxations are called: α_{EB} and α_{PS} respectively, in an increasing order of temperature.

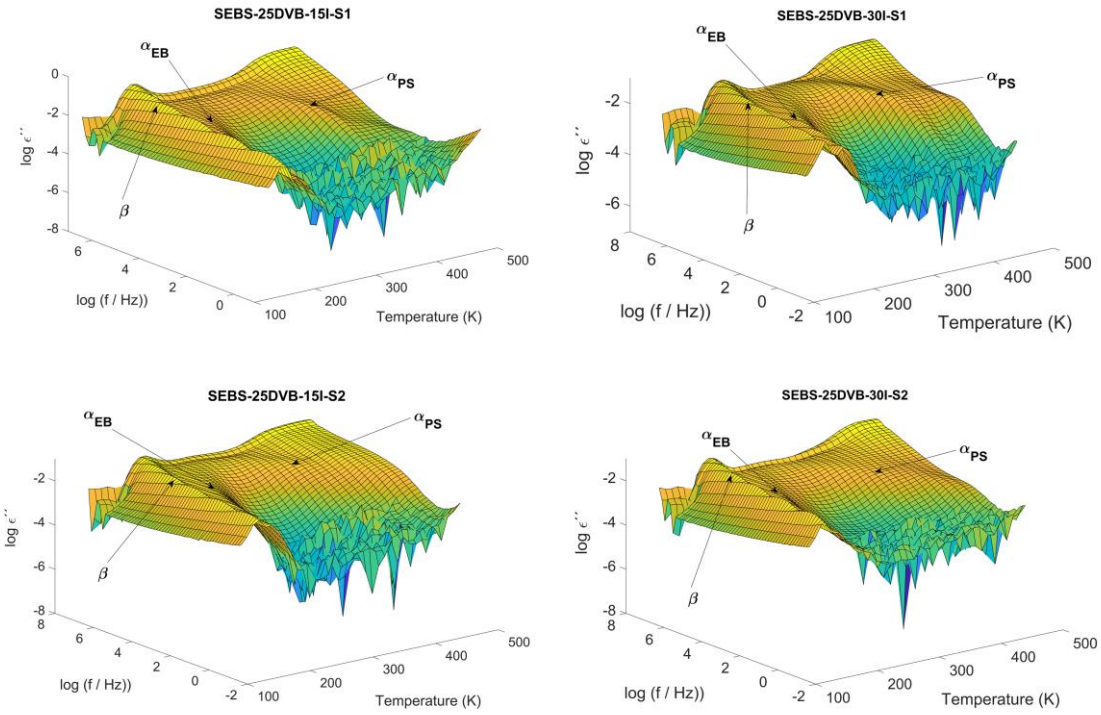

Figure 2

In accordance with previous works, [20,21,31] α_{EB} y α_{PS} relaxations can be attributed to the glass transition because the temperature peaks of each relaxation are in agreement with the DSC measurements to the poly(ethylene-butylene) (PEB) and poly(styrene) (PS) blocks, respectively [17,32].

As previous results show [17], when the neat SEBS was mixtured with DVB and photocrosslinked, the DSC measurements display a lack of variations of the PEB block, whereas in the PS block, the glass transition temperature of the non-irradiated copolymers is higher than the irradiated ones. In SEBS-25DVB without photocrosslinking, the glass transition temperature is 213 K and 445 K for the PEB and PS phase, respectively. However, in the SEBS-25DVB-15I with photocrosslinking, these temperatures are 213 K and 335 K for the PEB and PS phase, respectively. It seems that the photocrosslinking only acts on the PS phase. On the other hand, the sulfonation may decrease the glass transition temperature of each block. However, the

temperature peaks of the β and α dielectric relaxations have a more complex behaviour as a consequence of photocrosslinking and sulfonation. Thus, the real effect is more difficult to understand than the DSC results describe [17].

To understand the effect of photocrosslinking and sulfonation on the molecular mobility of each block, the dielectric relaxation spectra were adjusted using the empirical Havriliak–Negami (HN) functions. The relaxation spectra were obtained adding so many functions as necessary, to represent each of the relaxations. Thus, all the characteristic parameters of each relaxation process were determined. The relaxation time τ, the values of the dielectric intensity or relaxation strength $\Delta\varepsilon$, and a, b parameters were also calculated. A general review of the parameters indicates that the values of all relaxations increase on increasing temperature. However, each one of these parameters can be affected by the photocrosslinking and sulfonation and were analyzed separately for each one of the relaxations afterwards.

Figure 3 displays the isothermal dielectric relaxation spectra, in terms of the real (ε') component of the complex dielectric permittivity (ε^*) at the frequency range $f = 10^{-2}$ - 10^7 Hz at several temperatures. The membranes studied are the neat SEBS, the mixture of SEBS with DVB copolymer (SEBS-25DVB), the mixture with DVB and photocrosslinking SEBS copolymers (SEBS-25DVB-15I and SEBS-25DVB-30I) and the mixture with DVB photocrosslinked and sulfonated SEBS copolymers (SEBS-25DVB-15I-S1, SEBS-25DVB-15I-S2, SEBS-25DVB-30I-S1 and SEBS-25DVB-30I-S2).

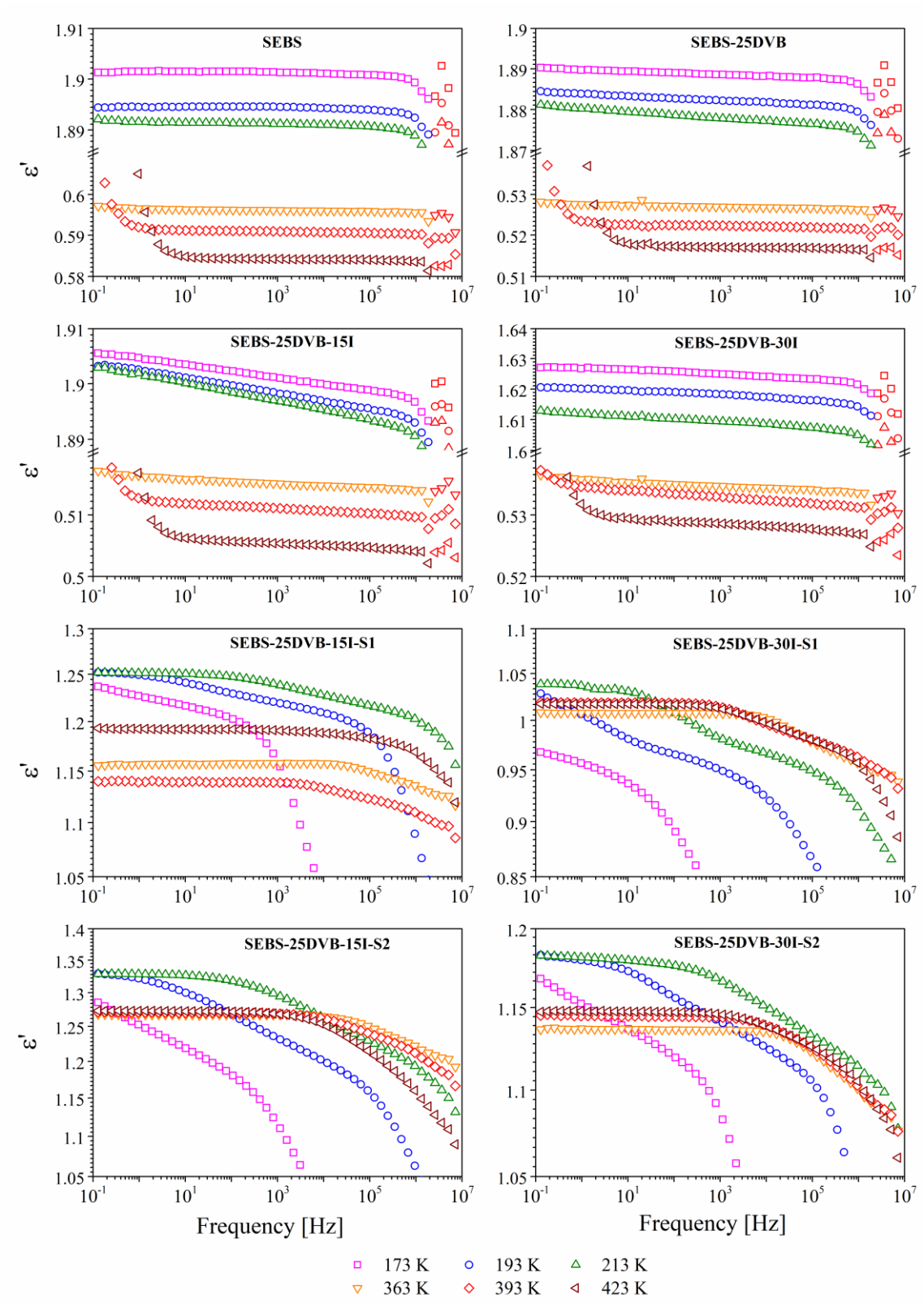
SEBS
SEBS-25DVB
SEBS-25DVB-15I
SEBS-25DVB-30I
SEBS-25DVB-15I-S1
SEBS-25DVB-30I-S1
SEBS-25DVB-15I-S2
SEBS-25DVB-30I-S2
ε'
Frequency [Hz]
173 K
193 K
213 K
363 K
393 K
423 K

Figure 3.

In this **Figure 3**, it is possible to observe the isothermal ε' values at low temperature for the neat SEBS and SEBS-25DVB copolymer. These values seem to slightly decrease between low to high frequencies, because in these intervals of temperatures and frequencies the movements of the molecular chains, of the poly(ethylene-butylene) PEB and the poly(styrene), PS block, are not present. In fact, the wide range between the temperature of the glass transition corresponding to the PEB and PS blocks, does not contribute to visualize both relaxations in the same frequency range. At high temperature, the isothermal ε' values slowly and continuously decrease with increasing frequency, because the dipoles will hardly be able to orient themselves in the direction of the applied field in the high frequency range.

The ε' isothermal curves analysed of the photo-reticulated SEBS-25DVB-15I and SEBS-25DVB-30I copolymer display a similar pattern the neat SEBS and SEBS-25DVB copolymer. However, the ε' values slightly decrease by photocrosslinking effect. This can be understood in terms of crosslinking, the interfacial properties, and the compatibility between the components of these copolymers. It has been observed in other polymers [33], that the crosslinking prevents the movement in the chains and shows a lower dielectric relaxation response.

Unlike the previous cases, the isothermal curves of the ε' of the photocrosslinked and sulfonated copolymers (SEBS-25DVB-15I-S1, SEBS-25DVB-15I-S2, SEBS-25DVB-30I-S1 and SEBS-25DVB-30I-S2) show~~s~~ several plateaus which are associated with the relaxation zones observed in **Figure 2**. The sulfonation may decrease the glass transition temperature of each block. Thus, it is also possible to observe that the value of the real ε' rapidly decreases due to the tendency of dipoles to orient themselves in the direction of the applied field.

In order to understand the intermolecular or intramolecular movements of each relaxation, the temperature dependence of the relaxation times was analysed by means of the Eyring model. The linear relationships between the relaxation times τ and the inverse of temperature were~~as~~ used to determine in a first approximation the apparent

activation energy. Thus, the **Figure 4** shows that for all the SEBS based copolymers described in **Table 1**, the experimental apparent activation energies *Ea*, for each one of the relaxations, were plotted versus the temperature corresponding to the dielectric loss factor obtained at a frequency of 1 Hz [34,35].

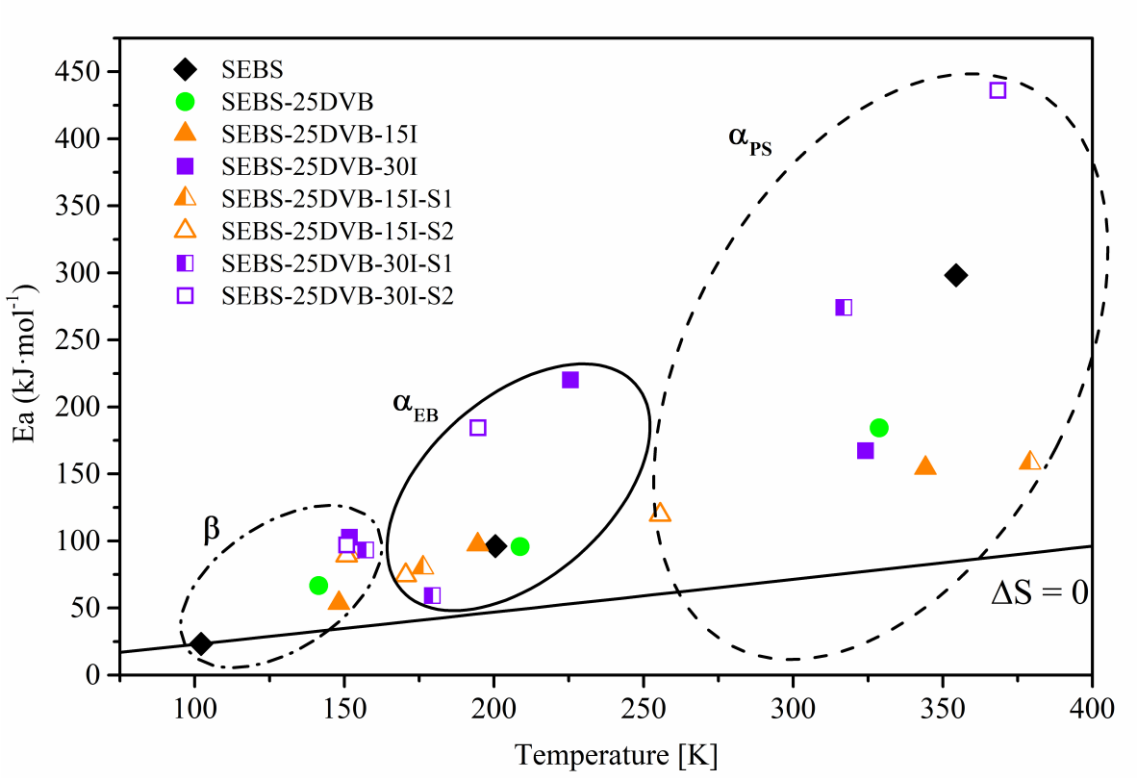

Figure 4

For all the SEBS based copolymers, the β relaxation has a low energy with a linear relationship with the temperature, which corresponds to an intramolecular movement. Photocrosslinking and subsequent sulfonation scarcely affect this relaxation being that a few carbon atoms are involved in this molecular movement. At higher temperatures, related to the glass transitions of both components of the block copolymer ethylene-butylene and styrene, the two high-energy relaxations were located. These relaxations were assigned to an intermolecular movement because all activation energies are clearly separated from linearity. In **Figure 4** seems that photocrosslinking and sulfonation affect a greater extent to the block of styrene than ethylene-butylene block, in agreement with DSC results. The copolymer SEBS-25DVB-30I-S2 is the most affected because it

has the highest concentration of SO_3H groups attached to benzene rings of styrene block that could increase the interaction between them.

In order to confirm the hypothesis of intra- or inter- macromolecular movement raised by the Eyring criterion, the dielectric behaviour of the copolymers was analysed by means of the Arrhenius plots, which consider the temperature-frequency interdependence for the maxima of loss factor isochrones. **Figure 5** shows the Arrhenius map for each of the relaxations of all SEBS based copolymers studied, where the β, α_{EB}, and α_{PS} relaxation zones are plotted. The lineal relationship between the relaxation times τ and the temperature of β relaxation proves this intramolecular origin. Thus, the thermal activation was characterised by means of Arrhenius equation. On the other hand, the nonlinear dependence between $log\ f$ *and* T^{-1} of the α_{EB}, and α_{PS} relaxations is representative of Vogel-Fulcher-Tamman-Hesse function, inherent of intermolecular movements.

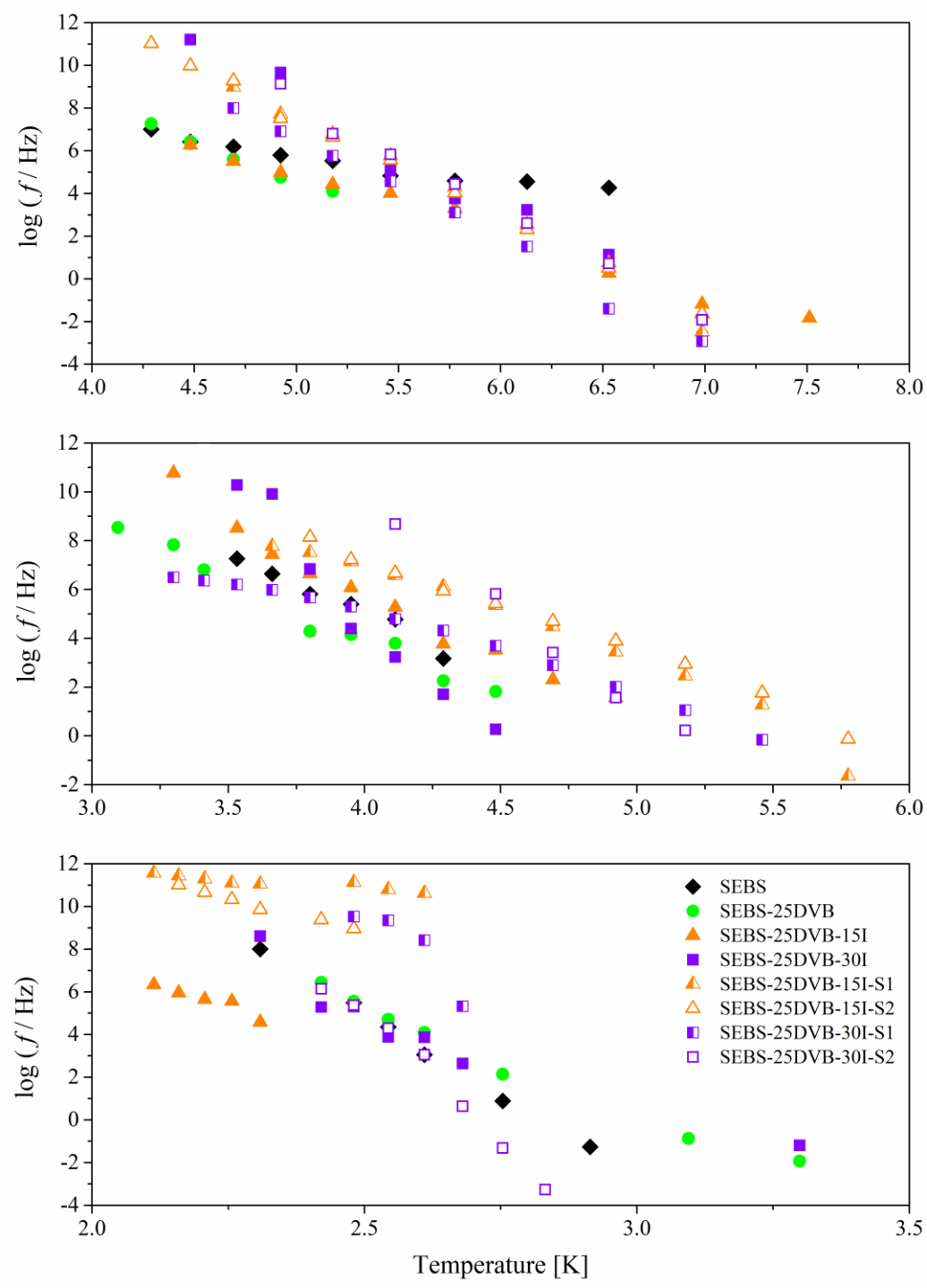
log (f / Hz)
Temperature [K]
SEBS
SEBS-25DVB
SEBS-25DVB-15I
SEBS-25DVB-30I
SEBS-25DVB-15I-S1
SEBS-25DVB-15I-S2
SEBS-25DVB-30I-S1
SEBS-25DVB-30I-S2

Figure 5

3.1 Low temperature local modes of molecular motions: β dielectric relaxation.

The zone of β dielectric relaxation appears in the temperature range of 166-184 K at the frequency of 1Hz. This relaxation is observed in the mechanical spectrum, but not all authors have been able to determine it [20].

Figure 6 exhibits how the loss dielectric permittivity varies due to the effect of photocrosslinking and subsequent sulfonation. As expected, the reticulation hinders the molecular movement and the shape of the relaxation widens, due to the different environments of the carbons involved in the movement within the same molecule. However, what really affects the shape of relaxation is sulfonation. The sulfonated copolymers (SEBS-25DVB-15I-S1, SEBS-25DVB-15I-S2, SEBS-25DVB-30I-S1 and SEBS-25DVB-30I-S2) have the same shape and only the SEBS-25DVB-30I-S1 appears at slightly higher temperatures. The Havriliak-Negami *a, b* parameters, were calculated for each copolymer.

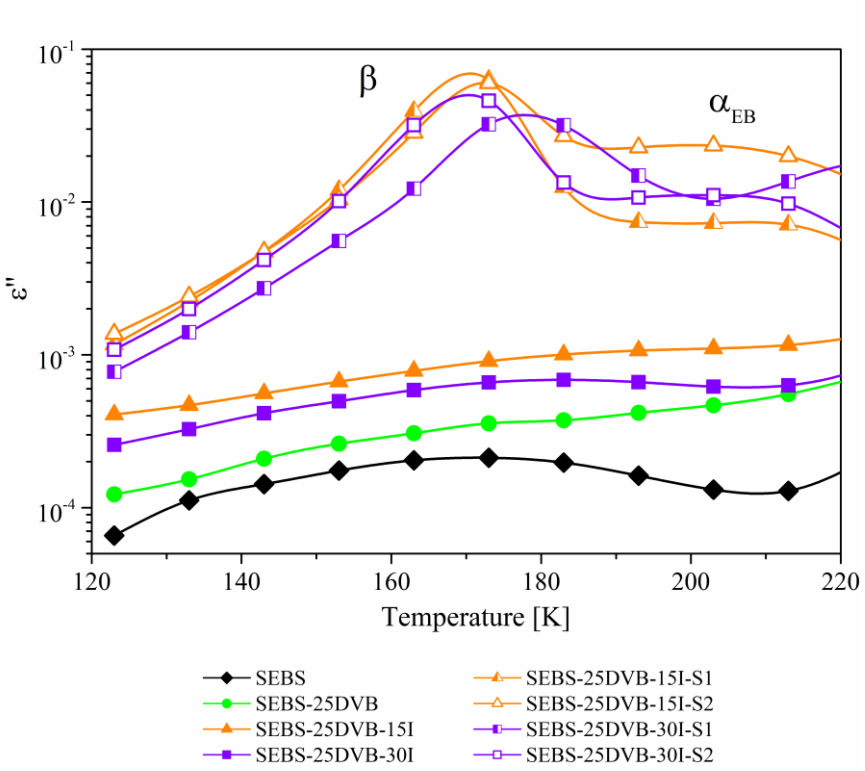

Figure 6

Figure 7 displays the parameter *a*, which is related to the width of β relaxation. It shows a linear increase with the temperature, for neat and photocrosslinking SEBS copolymers, as is normally found for similar β relaxation [21].

The sulfonation increases the values of the parameter *a*, of all the sulfonated copolymers and lie in the range 0.8−0.95. The closeness of this parameter to the unit suggests the narrow distribution of relaxation time for the β relaxation. **Figure7** also shows the parameter *b* which values are around 0.1−0.8, they increase with the sulfonation, and it seems that are slight dependent on the temperature.

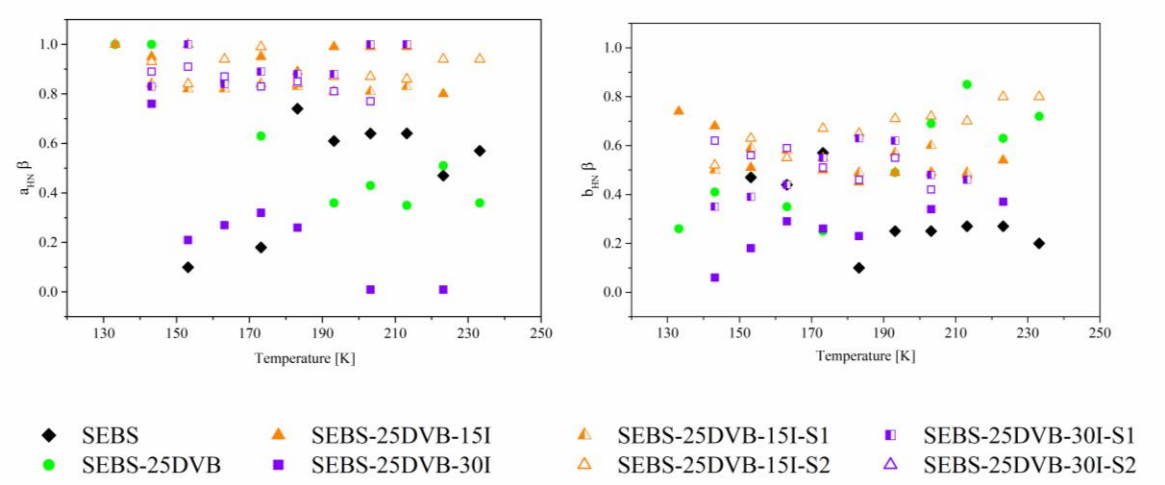

Figure 7

The values of the dielectric strength $\Delta\varepsilon$ of the β relaxation were also calculated and are displayed in **Table 2**. As it is expected, the strength values increase with the addition of DVB, but decrease with the crosslinking. However, the biggest increment is produced by the sulfonation although these values do not increase linearly. The 25DVB-30I-S1 membrane has a higher value than membranes more sulfonated. This is a significant result that seems to indicate that a lineal increase of the sulfonation does not necessarily imply a linear increase in the number of atoms with the ability to move.

Table 2

T (K)	SEBS	SEBS-25DVB	SEBS-25DVB-15I	SEBS-25DVB-30I	SEBS-25DVB-15I-S1	SEBS-25DVB-15I-S2	SEBS-25DVB-30I-S1	SEBS-25DVB-30I-S2
153	0,0013	0,0036	0,0023	0,0148	0,2122	0,1399	0,4731	0,2080
163	0,0015	0,0056	0,0002	0,0095	0,1828	0,1127	0,1351	0,1610
173	0,0016	0,0061	0,0043	0,0090	0,1711	0,0975	0,1470	0,1841

Table 3 displays the characteristic parameters of the Arrhenius model for all copolymers. The values of the apparent activation energy *Ea* obtained for the copolymer SEBS is 23 kJ·mol^{-1}. When DVB is added to SEBS copolymer the apparent activation energy increases. The value for SEBS-25DVB is 69 kJ·mol^{-1}. In both cases, these values would be characteristic of the reorientation movements of small angles of the carbons that take part of the chain movement in relation to the longitudinal axis of the polymer. Thus, the β dielectric relaxation would be associated with an intramolecular local mobility of small number of atoms of butylene backbone [21] or lateral ethyl group, which are not affected by the presence of the styrene block phase.

Table 3

	SEBS	SEBS-25DVB	SEBS-25DVB-15I	SEBS-25DVB-30I	SEBS-25DVB-15I-S1	SEBS-25DVB-15I-S2	SEBS-25DVB-30I-S1	SEBS-25DVB-30I-S2
Ea (kJ·mol^{-1})	23.2	68.8	53.6	102.7	91.6	89.1	93.2	97.0
1kHz Tmax (K)	137	184	176	166	167	167	174.0	165.5
R^2	0.932	0.996	0.993	0.987	0.995	0.999	0.997	0.996

The photocrosslinking decreases the apparent activation energy of SEBS-25DVB copolymers for lower doses SEBS-25DVB-15I and increases these values for longer UV irradiation while the sulfonation barely affects.

All these results indicate that the molecular movement associated with relaxation is a localized movement within the same molecule with a very narrow relaxation time. The

crosslinking produces a three-dimensional structure, which maintains the apparent activation energy around 90 kJ·mol^{-1} after the sulfonation. However, the sulfonation of the PS block modifies the intensity of the β-relaxation, although this movement occurs in the PEB block.

3.2 High temperature local modes of molecular motions: α_{EB}, α_{PS} dielectric relaxations

As mentioned above, the α-relaxation zone is associated with long-range chain segmental mobility of block copolymers and is possible to distinguish two glass transitions corresponding to each one of the blocks. The dielectric relaxation is caused by the cooperative backbone movements in each of the two phases of segregated block copolymers and have the peculiar characteristics of each block [20,36–39]. Thus, dielectric spectrum of SEBS presents two well-separated peaks, one at lower temperatures due to a segmental relaxation in the PEB block domains and other at higher temperature assigned to segmental relaxation in the PS block domains. As the photocrosslinking and the sulfonation have different effect on each relaxation, they were studied separately.

3.2.1 α_{EB} dielectric relaxation

Figure 8 shows the loss permittivity as a function of temperature for the α_{EB} relaxation. The α_{EB} relaxation peak appears between 225 and 250 K. In this case, significant modifications can be seen due to the photoirradiation or sulfonation of the membranes. The width and the temperature values of α_{EB} relaxation peak increase with the photocrosslinking although it depends on the exposure time. Once the copolymer was sulfonated the loss permittivity value increases significantly and the temperature value of α_{EB} relaxation peak decreases again, but a linear relationship is not established. This behaviour could be interpreted in terms of the heterogeneity of the ethylene-butylene block. Chains form aggregates where predominantly one or the other copolymer prevails and interphase zones must be produced, where the properties of the copolymer vary significantly. The molecular chains of sulfonated membranes start to move at

lower temperatures but the *SEBS-25DVB-30I-S1* membrane has a particular behaviour, which needs to be analysed.

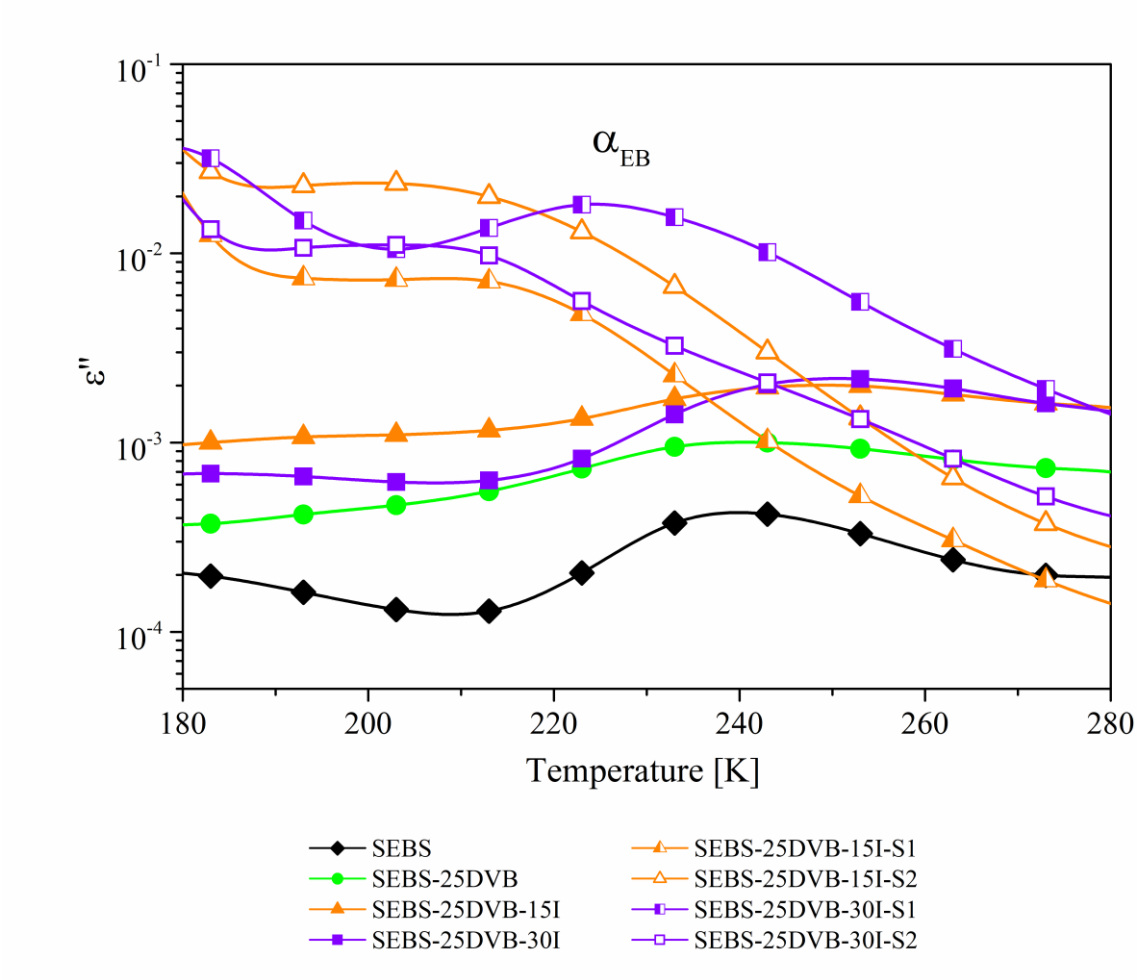

Figure 8

In order to characterize this relaxation, a deep analysis of the Havriliak-Negami parameters, such as the shape parameters; dielectric strength and the relationship between the relaxation times and the temperature, were also calculated.

The *a* and *b* parameters, which are related to the shape of the α_{EB} relaxation, are shown in **Figure 9.** The *a* parameter decreases with the temperature and the *b* parameter show less pronounced variation. These results agree with those obtained by other authors, which suggested the fluctuations in local dipole concentrations [21]. The *SEBS-25DVB-30I-S1* membrane has the highest values indicating a particular behaviour.

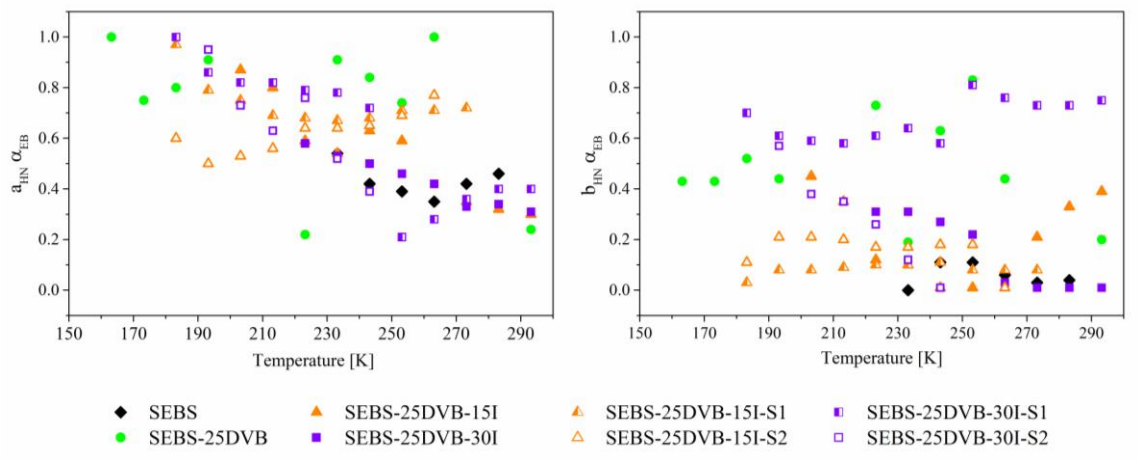

Figure 9

Table 4 shows the $\Delta\varepsilon$ parameter, related to the width α_{EB} relaxation, which increases with the degree of photocrosslinking and with the sulfonation. The *SEBS-25DVB-30I-S1* membrane has the lowest values among all the sulfonated membranes.

Table 4

T (K)	SEBS	SEBS-25DVB	SEBS-25DVB-15I	SEBS-25DVB-30I	SEBS-25DVB-15I-S1	SEBS-25DVB-15I-S2	SEBS-25DVB-30I-S1	SEBS-25DVB-30I-S2
223	0,0035	0,0014	0,0062	0,0131	0,1039	0,1769	0,0722	0,1804
233	0,0032	0,0014	0,0185	0,0204	0,1175	0,1741	0,0666	0,0548
243	0,0031	0,0003	0,1140	0,0230	0,1101	0,1140	0,0681	0,3224

Table 5 displays the characteristic parameters obtained by adjusting the experimental data to the VFTH model. The values of T_V, typically appears around 50 K below the glass transition temperature for the poly-ethylene-butylene block, decreases by the effect of both photocrosslinking and sulfonation. The parameter *D* is a non- dimensional factor related to the topology of the theoretical potential energy surface of the system and is calculated from T_V as $B = D \cdot T_V$. In the photocrosslinked membranes the *D* parameter increases, and clearly decreases with the sulfonation. The free volume coefficient Φ could visualize the change in cooperative movement. The photocrosslinking reduced the free volume as it was expected. The *SEBS-25DVB-30I-S1* membrane has more free volume coefficient that the other sulfonated membranes. These results could be explained due to the PEB domains are coupled by covalent interactions

with the PS domains, so that, what happens in the PS domains should affect the PEB domains to some degree. The attachment of SO_3H groups on the PS blocks not only change cohesion in these crosslinked domains but also perturb chain conformations in the PEB region causing a decrease of their T_g. The more free volume, the less energy to overcome the α_{EB} relaxation.

Table 5

	T_g (K)	log (τ_0/Hz)	D_0	T_v (K)	Φ_g/ B	α_f x 10^4 (K^{-1})	R^2
SEBS	227.9	10.14 ± 1.03	4.79 ± 2.41	177.89 ±14.79	0.059	11.733	0.993
SEBS-25DVB	224.9	12.54±0.44	7.89 ± 1.38	174.89 ± 5.86	0.036	7.258	1.000
SEBS-25DVB-15I	170.0	30.39 ± 1.16	68.06 ± 3.88	120.00 ± 0.00	0.006	1.224	0.990
SEBS-25DVB-30I	171.2	30.36 ± 1.43	61.13 ± 3.84	121.20 ± 0.00	0.007	1.350	0.958
SEBS-25DVB-15I-S1	170.7	12.62 ± 0.66	14.08 ± 2.89	120.65 ± 6.09	0.029	5.886	0.995
SEBS-25DVB-15I-S2	122.1	16.49 ± 1.90	52.94±31.85	72.14 ± 20.74	0.013	2.619	0.993
SEBS-25DVB-30I-S1	166.0	9.59 ± 0.42	13.10 ± 2.62	116.02 ± 6.99	0.033	6.579	0.995
SEBS-25DVB-30I-S2	159.4	12.87 ± 0.39	17.19 ± 1.97	109.43 ± 3.34	0.027	5.317	0.998

3.2.2 α_{PS} dielectric relaxation

Figure 10 shows the *ε''* relaxation between 375 and 425 K. The photocrosslinking or sulfonation of the membranes slightly increases the temperature peak. Only the height of the α_{PS} dielectric relaxation progressively increases depending on the exposure time and the degree of sulfonation. The highest values corresponds to *SEBS-25DVB-30I-S1* membrane, despite not being the most sulfonated. This behaviour could be unexpected because SO_3H groups are linked to the phenyl ring of styrene block, and thus, it could be guessed that an increment will be found if the dipole moment per unit volume increases. However, it seems that the phenyl group could add restrictions on PS block if the number of these dipole is high. In addition, the shape of the α_{PS} dielectric relaxation indicates more homogeneity in the styrene block than that observed in the ethylene-butylene block.

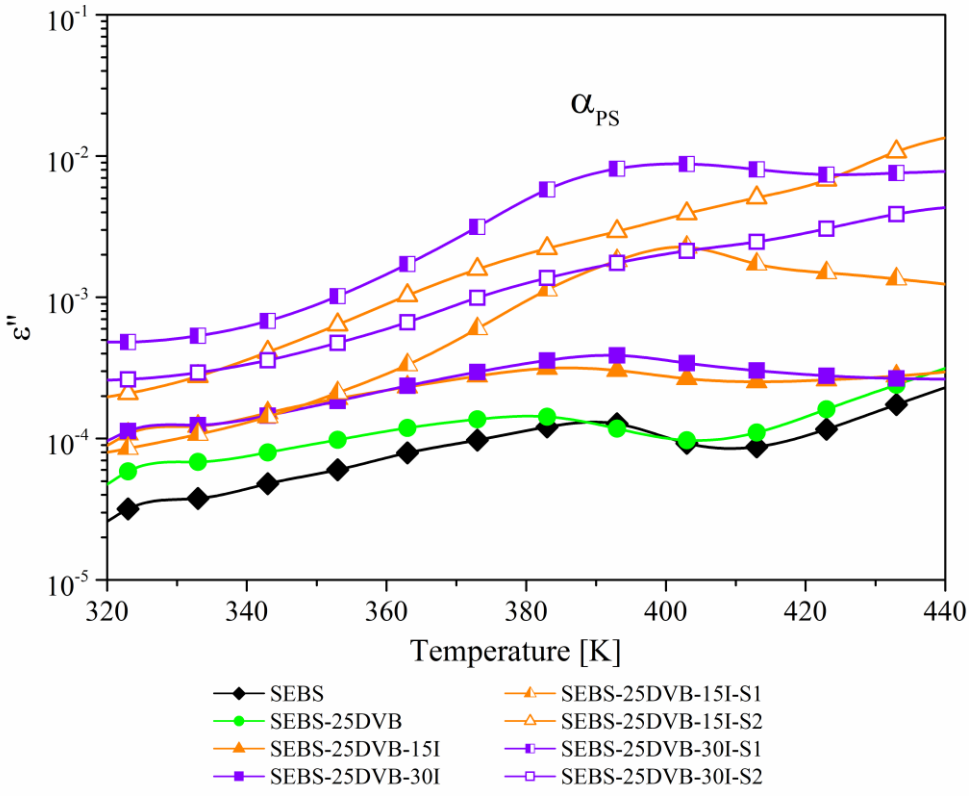

Figure 10

Again, in order to characterize this relaxation the following Havriliak-Negami parameters, shape parameters; dielectric strength and the relationship between the relaxation times and the temperature, were determined.

The *a* and *b* parameters are shown in **Figure 11.** Both parameters slightly depend on the temperature. The *a* parameter is closer to 1 for the photocrosslinked membranes and near to 0.5 for sulfonated ones. However, the *b* parameter is closer to 1 for the sulfonated membranes and near to 0.4 to the photocrosslinked ones.

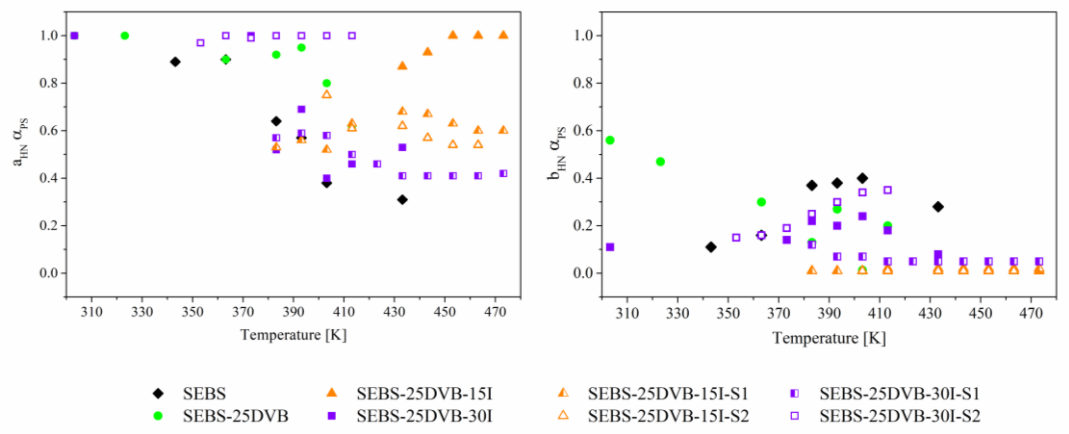

Figure 11

Table 6 displays the *Δε* parameters which increase with the degree of photocrosslinking and sulfonation. The *SEBS-25DVB-15I-S1 and SEBS-25DVB-15I-S2* membranes have the highest values among all the sulfonated membranes. The reason for the prominent loss was contributed to the strong proton/charge conducting ability of the SO_3H groups on the sulfonated styrene blocks, leading to the dissipation of the charges within the sSEBS [8].

Table 6

T (K)	SEBS	SEBS-25DVB	SEBS-25DVB-15I	SEBS-25DVB-30I	SEBS-25DVB-15I-S1	SEBS-25DVB-15I-S2	SEBS-25DVB-30I-S1	SEBS-25DVB-30I-S2
383	0,0013	0,0022	0,0122	0,0036	2,3510	5,4860	0,2202	0,0118
393	0,0008	0,0008	0,0122	0,0052	3,4020	5,8380	0,7015	0,0092
403	0,0011	0,0011	0,0105	0,0046	4,8590	5,6270	1,1110	0,0080

Table 7 shows the values of the adjustment parameters to the VFTH model for α_{PS} relaxation. The *Tv* calculated from the VFTH model for the polystyrene block increases significantly due to photocrosslinking, although it depends on the exposure time. Nevertheless, once the copolymer has been crosslinked, if it undergoes a sulfonation, the *Tv* value decreases again. Similarly, the coefficient of expansion values increase with crosslinking and decrease with sulfonation, but it is not possible to establish a linear relationship that points out both effects.

Table 7

	Tg (K)	log (τ_0/Hz)	D0	Tv(K)	Φg/ B	α_f x 10^4 (K^{-1})	R^2
SEBS	319.3	19.30 ± 0.60	15.81 ± 1.74	269.33 ± 5.86	0.012	2.348	1
SEBS-25DVB	260.0	18.44 ± 11.97	27.35 ± 62.54	210.03±136.86	0.009	1.741	0.991
SEBS-25DVB-30I	353.2	10.14 ± 9.78	3.95 ± 14.55	303.19±133.60	0.042	8.339	0.828
SEBS-25DVB-15I-S2	380.8	14.90 ± 2.05	3.59 ± 3.85	330.84 ± 51.48	0.042	8.434	0.996
SEBS-25DVB-30I-S1	338.1	16.13 ± 3.07	7.60 ± 7.23	288.13 ± 45.65	0.023	4.567	0.931
SEBS-25DVB-30I-S2	309.2	21.81 ± 5.66	21.09 ± 14.56	259.21 ± 32.32	0.009	1.83	0.99

A tentative explanation could be related to the increasing restrictions on styrene block motions when rising the number of SO_3H groups which would lead to the formation of a sub-phase at higher sulfonation degrees. This would justify the largest vertical displacement observed between the curves for unsulfonated SEBS and the sulfonated series.

All these results could indicate that the attachment of SO_3H groups to the PS blocks changes the cohesion of the crosslinked domains but also perturbs chain conformations in the PEB region, which have a significant influence on the molecular movement, and consequently, on the relaxation spectrum of each one of these SEBS based membranes.

3.3 Proton conductivity measurements of UV irradiated and post-sulfonated SEBS-DVB membranes.

Through-plane proton conductivities of photocrosslinked and post-sulfonated membranes were measured at 333 K and 100% relative humidity in a fuel cell test station connected to a frequency response analyser. Contrary to what initially seemed foreseeable, the membranes subjected to a more intense sulfonation treatment (SEBS-25DVB-15I-S2 and SEBS-25DVB-30I-S2) showed lower conductivity as it is shown in **Figure 12.** These results are in total agreement with those obtained by the dielectric characterization since they had been already predicted a more severe restriction of mobility in the PS block when the number of phenyl groups functionalized with polar groups is considerably higher. This fact again probes that lineal increase of the sulfonation does not necessarily imply a linear increase in the number of atoms with the ability to move.

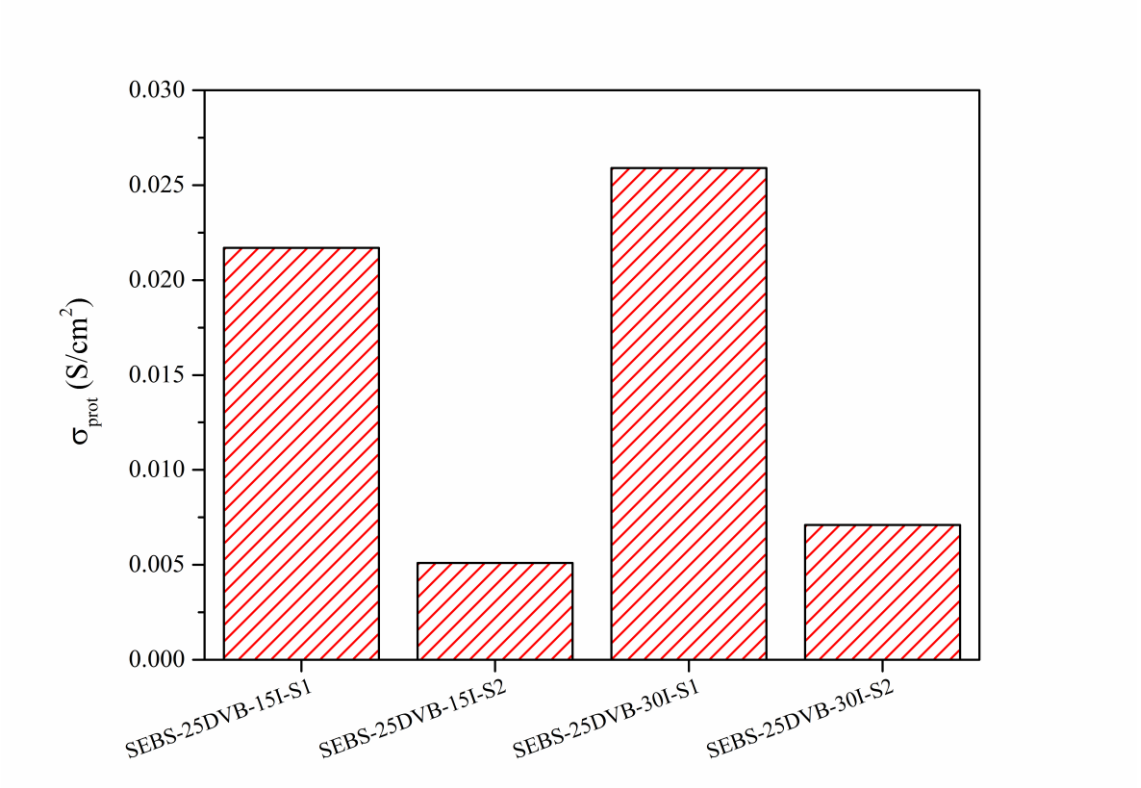
0.030
0.025
0.020
0.015
0.010
0.005
0.000
σprot (S/cm2)
SEBS-25DVB-15I-S1
SEBS-25DVB-15I-S2
SEBS-25DVB-30I-S1
SEBS-25DVB-30I-S2

Figure 12

4. Conclusions

The dielectric relaxation spectra of the neat *SEBS, SEBS-25DVB,* and photocrosslinked and sulfonated copolymer consist of: a weak β relaxation at low temperature attributed to the movement of few atoms from the main or the lateral chain of poly(ethylene-butylene) (PEB) block; and two α_{EB}, α_{PS} relaxations related to the glass transition of both ethylene-butylene and styrene blocks, respectively. The lineal thermal activation of the β relaxation indicates its intramolecular origin whereas the nonlinear thermal activation of the two α_{EB}, α_{PS} relaxations reveal their intermolecular origin.

The photocrosslinking and subsequent sulfonation slightly modify the apparent activation energy of the β relaxation. However, the loss dielectric permittivity increases with the degree of sulfonation which is an indication of a light influence of PS block on the movement of PEB chains.

Significant modifications are produced by the photocrosslinking and sulfonation processes on the α_{EB} relaxation, contrary to what was expected. The molecular chains of sulfonated membranes start to move at lower temperatures. The attachment of SO_3H groups on the PS blocks not only changes cohesion in these crosslinked domains but also perturbs chain conformations in the PEB region.

The photocrosslinking or sulfonation of the membranes progressively increases the height of α_{PS} dielectric relaxation depending on the exposure time and the degree of sulfonation. It seems that the phenyl group could add restrictions on the PS block if the number of sulfonic groups is high. In addition, the shape of the α_{PS} dielectric relaxation indicates more homogeneity in the PS block than that observed in the PEB block. The highest values correspond to *SEBS-25DVB-30I-S1* membrane, despite not being the most sulfonated. A lineal increase of the sulfonation does not necessarily imply a linear increase in the number of atoms with the ability to move.

According to the findings of dielectric analysis, the membrane with more free volume and more molecular mobility (SEBS-25DVB-30I-S1) is the one with the highest proton

conductivity. Thus, the comparative study of the dielectric relaxation spectrum of the membranes intended to function as electrolytes together with the analysis of their performance in low temperature fuel cells may constitute a helpful methodology to re-design these electrolytes and is the subject of future work.

5. Acknowledgments

The authors would like to thank the support of the European Union is through the European Regional Development Funds (ERDF) and the Spanish Ministry of Economy, Industry and Competitiveness, for the research projects POLYDECARBOCELL (ENE2017-86711-C3-1-R), REPICOMES (ENE2017-90932-REDT) and UPV- (PAID -10-19) SUB-1 grant for R. Teruel.

6. Data availability

The raw/processed data required to reproduce these findings cannot be shared at this time as the data also forms part of an ongoing study.

7. References

[1] T.R. Ralph, Principles of Fuel Cells, Platin. Met. Rev. 50 (2006) 200–201.
[2] J. Larminie, A. Dicks, M.S. McDonald, Fuel cell systems explained, J. Wiley Chichester, UK, 2003.
[3] R. O'hayre, S.-W. Cha, W. Colella, F.B. Prinz, Fuel cell fundamentals, John Wiley & Sons, 2016.
[4] N.R. Legge, Thermoplastic elastomers, Rubber Chem. Technol. 60 (1987) 83–117.
[5] C.H. Lee, H.B. Kim, S.T. Lim, H.S. Kim, Y.K. Kwon, H.J. Choi, Ordering behavior of layered silicate nanocomposites with a cylindrical triblock copolymer, Macromol. Chem. Phys. 207 (2006) 444–445.
[6] B. Kim, J. Kim, B. Cha, B.J.-J. of membrane science, undefined 2006, Effect of selective swelling on protons and methanol transport properties through partially sulfonated block copolymer membranes, Elsevier.
[7] F. Brum, F. Zanatta, E. Marczynski, M.F.-S.S. Ionics, undefined 2014, Synthesis and characterisation of a new sulphonated hydrocarbon polymer for application as a solid proton-conducting electrolyte, Elsevier.
[8] J.E. Yang, J.S. Lee, Selective modification of block copolymers as proton exchange membranes, in: Electrochim. Acta, 2004: pp. 617–620.
[9] A.R. Kim, M. Vinothkannan, M.H. Song, J.-Y. Lee, H.-K. Lee, D.J. Yoo, Amine functionalized carbon nanotube (ACNT) filled in sulfonated poly(ether ether ketone) membrane: Effects of ACNT in improving polymer electrolyte fuel cell performance under reduced relative humidity, Compos. Part B Eng. 188 (2020) 107890.
[10] K.H. Lee, J.Y. Chu, A.R. Kim, D.J. Yoo, Enhanced Performance of a Sulfonated Poly(arylene ether ketone) Block Copolymer Bearing Pendant Sulfonic Acid Groups for Polymer Electrolyte Membrane Fuel Cells Operating at 80% Relative Humidity, ACS Appl. Mater. Interfaces. 10 (2018) 20835–20844.
[11] J. Meier-Haack, A. Taeger, C. Vogel, K. Schlenstedt, W. Lenk, D. Lehmann, Membranes from sulfonated block copolymers for use in fuel cells, Sep. Purif. Technol. 41 (2005) 207–220.
[12] A. Ganguly, A.K. Bhowmick, Sulfonated styrene-(ethylene-co-butylene)-styrene/montmorillonite clay nanocomposites: Synthesis, morphology, and properties, Nanoscale Res. Lett. 3 (2008)
[13] A. Mokrini, C. del Río, J.L. Acosta, Synthesis and characterization of new ion conductors based on butadiene styrene copolymers, Solid State Ionics. 166 (2004) 375–381.
[14] C. del Río, J.R. Jurado, J.L. Acosta, Hybrid membranes based on block co-polymer ionomers and silica gel. Synthesis and characterization, Polymer (Guildf). 46 (2005) 3975–3985.
[15] A. Navarro, C. del Río, J.L. Acosta, Kinetic study of the sulfonation of hydrogenated styrene butadiene block copolymer (HSBS): Microstructural and electrical characterizations, J. Memb. Sci. 300 (2007) 79–87.
[16] P.G. Escribano, C. del Río, J.L. Acosta, Preparation, characterization and single cell testing of new ionic conducting polymers for fuel cell applications, J. Power

Sources. 187 (2009) 98–102.
[17] C. del Río, O. García, E. Morales, P.G. Escribano, Single cell performance and electrochemical characterization of photocrosslinked and post-sulfonated SEBS-DVB membranes, Electrochim. Acta. 176 (2015) 378–387.
[18] R. Teruel Juanes, Propiedades dieléctricas y conductividad de nuevos electrolitos poliméricos para aplicaciones energéticas., Universitat Politècnica de València, 2017.
[19] N. Ni, K. Zhao, Dielectric analysis of chitosan gel beads suspensions: Influence of low crosslinking agent concentration on the dielectric behavior, J. Colloid Interface Sci. 312 (2007) 256–264.
[20] H. Chen, M.K. Hassan, S.K. Peddini, K.A. Mauritz, Macromolecular dynamics of sulfonated poly (styrene-b-ethylene-ran-butylene-b-styrene) block copolymers by broadband dielectric spectroscopy, Eur. Polym. J. 47 (2011) 1936–1948.
[21] S. Cerveny, R. Bergman, G.A. Schwartz, P. Jacobsson, Dielectric α- and β-relaxations in uncured styrene butadiene rubber, Macromolecules. 35 (2002) 4337–4342.
[22] P. Atorngitjawat, R.J. Klein, J. Runt, Dynamics of sulfonated polystyrene copolymers using broadband dielectric spectroscopy, Macromolecules. 39 (2006) 1815–1820.
[23] N. Hadjichristidis, S. Pispas, G. Floudas, Block copolymers: synthetic strategies, physical properties, and applications, John Wiley & Sons, 2003.
[24] I. Alig, F. Kremer, G. Fytas, J. Roovers, Dielectric relaxation in disordered poly (isoprene-styrene) diblock copolymers near the microphase-separation transition, Macromolecules. 25 (1992) 5277–5282.
[25] E. Helal, N.R. Demarquette, L.G. Amurin, E. David, D.J. Carastan, M. Fréchette, Styrenic block copolymer-based nanocomposites: Implications of nanostructuration and nanofiller tailored dispersion on the dielectric properties, Polymer (Guildf). 64 (2015) 139–152.
[26] E. Helal, L.G. Amurin, D.J. Carastan, R.R. de Sousa Jr, E. David, M. Frechette, N.R. Demarquette, Interfacial molecular dynamics of styrenic block copolymer-based nanocomposites with controlled spatial distribution, Polymer (Guildf). 113 (2017) 9–26.
[27] H.A. Bolados, M. Hernández-Santana, L.J. Romasanta, M. Yazdani-Pedram, R. Quijada, M.A. López-Manchado, R. Verdejo, Electro-mechanical actuation performance of SEBS/PU blends, Polymer (Guildf). 171 (2019) 25–33.
[28] S. Havriliak, S. Negami, A complex plane representation of dielectric and mechanical relaxation processes in some polymers, Polymer (Guildf). 8 (1967) 161–210.
[29] S. Havriliak, S. Negami, A complex plane analysis of α-dispersions in some polymer systems, in: J. Polym. Sci. Part C Polym. Symp., Wiley Online Library, 1966: pp. 99–117.
[30] J.M. Charlesworth, Deconvolution of overlapping relaxations in dynamic mechanical spectra, J. Mater. Sci. 28 (1993) 399–404.
[31] N. Miura, W. MacKnight, S. Matsuoka, F.K.- Polymer, undefined 2001, Comparison of polymer blends and copolymers by broadband dielectric analysis, Elsevier.
[32] S. Yuan, C. del Rio, M. López-González, X. Guo, J. Fang, E. Riande, Impedance

spectroscopy and performance of cross-linked new naphthalenic polyimide acid membranes, J. Phys. Chem. C. 114 (2010) 22773–22782.

[33] A.R. Blythe, T. Blythe, D. Bloor, Electrical properties of polymers, Cambridge university press, 2005.
[34] H. Eyring, The activated complex in chemical reactions, J. Chem. Phys. 3 (1935) 107–115.
[35] J. Heijboer, Molecular origin of relaxations in polymers, Ann. N. Y. Acad. Sci. 279 (1976) 104–116.
[36] A. Kyritsis, P. Pissis, S.-M. Mai, C. Booth, Comparative Dielectric Studies of Segmental and Normal Mode Dynamics of Poly (oxybutylene) and Poly (oxyethylene)− Poly (oxybutylene) Diblock Copolymers, Macromolecules. 33 (2000) 4581–4595.
[37] I. Alig, G. Floudas, A. Avgeropoulos, N. Hadjichristidis, Junction Point Fluctuations in Microphase Separated Polystyrene− Polyisoprene− Polystyrene Triblock Copolymer Melts. A Dielectric and Rheological Investigation, Macromolecules. 30 (1997) 5004–5011.
[38] R. Lund, L. Willner, A. Alegría, J. Colmenero, D. Richter, Self-concentration and interfacial fluctuation effects on the local segmental dynamics of nanostructured diblock copolymer melts, Macromolecules. 41 (2008) 511–514.
[39] C. Lorthioir, A. Alegria, J. Colmenero, B. Deloche, Heterogeneity of the segmental dynamics of poly (dimethylsiloxane) in a diblock lamellar mesophase: dielectric relaxation investigations, Macromolecules. 37 (2004) 7808–7817.

8. Figure Captions

Figure 1. Chemical structure of SEBS-based membranes.

Figure 2. Dielectric relaxation spectrum of styrene-ethylene-butylene-styrene SEBS-25DVB-15I-S1, SEBS-25DVB-15I-S2, SEBS-25DVB-30I-S1and SEBS-25DVB-30I-S2.

Figure 3. Isothermal curves of the real ε' component of the complex dielectric permittivity ε* of styrene-ethylene-butylene-styrene copolymers SEBS, SEBS-25DVB, SEBS-25DVB-15I, SEBS-25DVB-30I, SEBS-25DVB-15I-S1, SEBS-25DVB-15I-S2, SEBS-25DVB-30I-S1and SEBS-25DVB-30I-S2.

Figure 4. Eyring plots of all the relaxations of styrene-ethylene-butylene-styrene copolymers SEBS, SEBS-25DVB, SEBS-25DVB-15I, SEBS-25DVB-30I, SEBS-25DVB-15I-S1, SEBS-25DVB-15I-S2, SEBS-25DVB-30I-S1 and SEBS-25DVB-30I-S2.

Figure 5. Arrhenius map of the (Top) β, (Middle) α_{EB}, (Bottom) α_{PS} for the SEBS, SEBS-25DVB, SEBS-25DVB-15I, SEBS-25DVB-30I, SEBS-25DVB-15I-S1, SEBS-25DVB-15I-S2, SEBS-25DVB-30I-S1 and SEBS-25DVB-30I-S2.

Figure 6. β-relaxation of all the relaxation of styrene-ethylene-butylene-styrene copolymers SEBS, SEBS-25DVB, SEBS-25DVB-15I, SEBS-25DVB-30I, SEBS-25DVB-15I-S1, SEBS-25DVB-15I-S2, SEBS-25DVB-30I-S1and SEBS-25DVB-30I-S2.

Figure 7. a and b Havriliak-Negami parameters of the *β*-relaxation for the styrene-ethylene-butylene-styrene copolymers SEBS, SEBS-25DVB, SEBS-25DVB-15I, SEBS-25DVB-30I, SEBS-25DVB-15I-S1, SEBS-25DVB-15I-S2, SEBS-25DVB-30I-S1and SEBS-25DVB-30I-S2.

Figure 8. α_{EB} – relaxation of the copolymers of styrene-ethylene-butylene-styrene SEBS, SEBS-25DVB, SEBS-25DVB-15I, SEBS-25DVB-30I, SEBS-25DVB-15I-S1, SEBS-25DVB-15I-S2, SEBS-25DVB-30I-S1and SEBS-25DVB-30I-S2.

Figure 9. a and b Havriliak-Negami parameters *of* α α_{EB}-relaxation of styrene-ethylene-butylene-styrene copolymers SEBS, SEBS-25DVB, SEBS-25DVB-15I, SEBS-25DVB-30I, SEBS-25DVB-15I-S1, SEBS-25DVB-15I-S2, SEBS-25DVB-30I-S1and SEBS-25DVB-30I-S2.

Figure 10. α_{PS}-relaxation of copolymers of styrene-ethylene-butylene-styrene SEBS, SEBS-25DVB, SEBS-25DVB-15I, SEBS-25DVB-30I, SEBS-25DVB-15I-S1, SEBS-25DVB-15I-S2, SEBS-25DVB-30I-S1 and SEBS-25DVB-30I-S2.

Figure 11. a and b Havriliak-Negami parameters of α_{PS}-relaxation of styrene-ethylene-butylene-styrene copolymers SEBS, SEBS-25DVB, SEBS-25DVB-15I, SEBS-25DVB-30I, SEBS-25DVB-15I-S1, SEBS-25DVB-15I-S2, SEBS-25DVB-30I-S1and SEBS-25DVB-30I-S2.

Figure 12. In situ through-plane proton conductivity at 60ºC and 100% relative humidity of SEBS-25DVB-15I-S1, SEBS-25DVB-30I-S1, SEBS-25DVB-15I-S2 and SEBS-25DVB-30I-S2.

9. Table Captions

Table 1: Nomenclature and composition of obtained SEBS-based membranes.

Table 2: Parameters of the dielectric strength of the β relaxation for SEBS-based membranes.

Table 3: Parameters of the Arrhenius equation for β relaxation for SEBS-based membranes.

Table 4: Parameters of the dielectric strength the α_{EB} relaxation for SEBS-based membranes.

Table 5: Parameters of the *Vogel-Fulcher-Tammann-Hesse* for α_{EB}-relaxation for SEBS-based membranes.

Table 6: Parameters of the dielectric strength the α_{PS} relaxation for SEBS-based membranes.

Table 7: Parameters of the *Vogel-Fulcher-Tammann-Hesse* for α_{PS}-relaxation for SEBS-based membranes.

R. Teruel-Juanes, B. Pascual-Jose, C. del Río, O. García, A. Ribes-Greus. Dielectric analysis of photocrosslinked and post-sulfonated styrene-ethylene-butylene-styrene block copolymer based membranes. Reactive and Functional Polymers 2020; 155:104715

OPEN ACCESS POLICIES